Advances in Aircraft and Spacecraft Science, *Vol. 10, No. 3 (2023) 281-302*
https://doi.org/10.12989/aas.2023.10.3.281

Bending analysis of exponentially varied FG plates using trigonometric shear and normal deformation theory

Sunil S. Yadav*, Keshav K. Sangle[a], Mandar U. Kokane,
Sandeep S. Pendhari[b] and Yuwaraj M. Ghugal[c]

Structural Engineering Department, *Veermata Jijabai Technological Institute*,
H.R Mahajani Marg, *Mumbai*, *400 019*, *Maharashtra*, *India*

(Received January 25, 2023, Revised April 26, 2023, Accepted June 20, 2023)

Abstract. In this paper, bending analysis of exponentially varying functionally graded (FG) plate is presented using trigonometric shear deformation theory (TSDT) considering both transverse shear and normal deformation effects. The in-plane displacement field consists of sinusoidal functions in thickness direction to include transverse shear strains and transverse displacement include the effect of transverse normal strain using the cosine function in thickness coordinate. The governing equations and boundary conditions of the theory are derived using the virtual work principle. System of governing equations, for simply supported conditions, Navier's solution technique is used to obtain results. Plate material properties vary across thickness direction according to exponential distribution law. In the current theory, transverse shear stresses are distributed accurately through the plate thickness, hence obviates the need for a shear correction factor. TSDT results are compared with those from other theories to ensure the accuracy and effectiveness of the present theory. The current theory is in excellent agreement with the semi-analytical theory.

Keywords: trigonometric shear deformation theory, exponential law, functionally graded plate

1. Introduction

The FGM is an enhanced composite where material properties vary gradually in the desired direction from one layer to another. The volume fractions of ingredient materials are paired continuously and smoothly due to location along a given domain direction of structure to obtain the ideal functioning and properties. The primary benefit of FG material is the removal of delamination failure at interfaces that occur with conventional laminated components when material properties change abruptly. Therefore, the FGM has numerous benefits compared to monolithic material and conventional laminated composites and sandwiches see Pradhan *et al.* (2019). Over the years, researchers have developed several theories to analyze the structural components of the FGM under different loading conditions such as mechanical, thermal and electrical loadings etc. Khan *et al.* (2019), Saleh *et al.* (2020) provided brief review of FGM and its analysis.

*Corresponding author, Ph.D. Student, E-mail: civiliansunil@gmail.com
[a]Professor, E-mail: kksangle@st.vjti.ac.in
[b]Professor, E-mail: sspendhari@st.vjti.ac.in
[c]Professor, E-mail: ymghugal@gmail.com

http://www.techno-press.org/?journal=aas&subpage=7 ISSN: 2287-528X (Print), 2287-5271 (Online)

FGMs are widely used in various fields such as aerospace, biomedical, energy industries, defense, marine, nuclear reactors, and optoelectronics. As FGM become increasingly common in structural elements, there is a need to developed mathematical models that can accurately predict their response under various loading conditions. Hence, various theories are developed to study the bending, buckling, and vibration behaviors of these elements.

Sankar (2001) provided an elasticity solution for the FG beam under transverse load with exponentially varying Young's modulus. The exponential distribution of elastic stiffness coefficients makes it possible to solve the elasticity equations precisely. Woodward and Kashtalyan (2011) developed a 3D elasticity equation for FG simply supported plates subjected to transverse loading. Lu (2008) used a state-space model to provide semi-analytical solutions for multidirectional FG plates using the differential quadrature method. Zhang *et al.* (2014) developed 3-D elasticity equations for the static bending of FG plates using a hybrid semi-analytical method called the state-space-based differential quadrature method. Using a variety of generalized-thermo-elasticity theories, Zenkour (2005) investigated the quasi-static bending behavior of a simply supported FG and exponentially varying plate subjected to a temperature field. Zhong *et al.* (2009) introduced the symplectic geometry technique to derive exact bending solutions for moderately thick rectangular plates with simply supported opposite edges. Garg *et al.* (2022) investigated the bending behavior of sandwich FGM beams under thermal loadings using shear deformation theory with temperature-dependent material properties. They considered the effects of different thermal profiles, power-law exponent and core thickness on the behavior of the beam.

To investigate elastic FG plates under transverse loads with a uniform Poisson's ratio and variable elastic moduli across thickness by a power law, exponential, and sigmoid laws, Chi and Chung (2006) used classical plate theory (CPT) and Fourier series expansion. Chakraverty and Pradhan (2014) used CPT and the Rayleigh-Ritz method to study the free vibration of FG rectangular plates with different boundary conditions. Using first-order shear deformation theory (FSDT), Chakraborty *et al.* (2003) analysed the thermo-elastic behavior of the FG beam. They considered the thickness as well as variable elastic and thermal properties. Nguyen *et al.* (2008) derived the transverse shear stress and shear correction factors for simply supported FG plates subjected to cylindrical bending. Pendhari *et al.* (2012) presented mixed semi-analytical, and analytical solutions for an FG simply supported rectangular plate. Bhandari and Purohit (2014) presented a bending analysis of FG plates using FEM subjected to uniform and point loads for variable volume fraction distributions and changing aspect ratios.

Praveen and Reddy (1998) used a finite element plate model to investigate the response of functionally graded (FG) ceramic-metal plates under Von-Karman type non-linearity, taking into account transverse shear strains, rotary inertia, and high rotations. Reddy (2000) presented a theoretical formulation, Navier's technique solutions, and a finite element models for the through-thickness analysis of FG plates based on third-order shear deformation theory (TOSDT). Shahrjerdi *et al.* (2011) investigated the vibration analysis of a rectangular FG plate using second-order shear deformation theory, using an energy method to derive equations of motion. Srividhya *et al.* (2018) used TOSDT to perform a nonlocal nonlinear analysis on FG plates subjected to static load. Bodaghi and Saidi (2010) applied higher-order shear deformation theory (HSDT) for buckling analysis of FG rectangular plate. Merdaci and Belghoul (2019) used HSDT with transverse normal deformation to examine the bending response of a porous FG thick rectangular plate. Na and Kim (2006) reported a nonlinear bending analysis of a simply supported FG rectangular plate under transverse loads based on Reddy's HSDT. Gulshan Taj *et al.* (2013) applied HSDT to investigate the static behavior of FG plates, assuming that transverse shear stresses are distributed quadratically throughout the plate's

thickness. Srividhya *et al.* (2019) formulated a generalised HSDT for the flexural analysis of FG plates subjected to UDL with varying intensities. Zenkour (2006) used generalised shear deformation theory to investigate the static behavior of a simply supported FG rectangular plate under the transverse uniform load.

Jha *et al.* (2013) employed higher-order shear and normal deformation theory (HOSNT) to investigate a static bending of rectangular FG plates subjected to transverse loading. Kant *et al.* (2014) presented static and dynamic analysis of FG simply supported plates using HOSNT. Meiche *et al.* (2011) applied four variable hyperbolic shear deformation theory for the static bending of FG rectangular plates. Nguyen (2015) used higher-order hyperbolic shear deformation theory for bending, buckling and free vibration analysis of FG plate using power and exponential laws. Gupta and Talha (2017) presented nonlinear flexural and vibrational analysis with geometric imperfections of FG plate based on hyperbolic shear and normal deformation theory.

Ghugal and Sayyad (2013) introduced trigonometric shear deformation theory (TSDT), which considers the transverse shear deformation and transverse normal strain effects. Sayyad and Ghugal (2017) developed a unified shear deformation theory for bending analysis of FG plate including the effect of transverse shear deformation using trigonometric, parabolic, exponential, and hyperbolic shape functions. Furthermore, Kulkarni *et al.* (2015) reported an analytical solution for static and buckling analysis of an FG plate by using the inverse TSDT. Swami and Ghugal (2021) presented analytical solutions for thick orthotropic laminated plates for linear and nonlinear thermal loads using TSDT, including transverse shear and normal strains, and thickness stretching effects. Yadav *et al.* (2022, 2023a, b) studied the bending response of FG beams and plates using TSDT with and without transverse normal effects. Sayyad and Ghugal (2016) examined cylindrical bending of laminated composite and sandwich plates using a sinusoidal shear and normal deformation plate theory that includes effects of transverse normal strain/deformation.

Several researchers (Bakoura *et al.* 2021, Guellil *et al.* 2021, Bouafia *et al.* 2021, Hachemi *et al.* 2021, Tahir *et al.* 2022, Zaitoun *et al.* 2022, Bennedjadi *et al.* 2023, Hadji *et al.* 2023) have reported the effect of porosity, material distribution, elastic foundation, geometry, and dimension ratios, on the bending, buckling, and vibration behavior of FG plates. Improved theories and numerical methods, such as the quasi-3D approach, mixed finite element method, and Hamilton's principle, have provided new insights into the behavior of advanced FGM plates under various loading conditions. Mudhaffar *et al.* (2021), Zaitoun *et al.* (2022) investigated the bending behavior of an FG ceramic-metal plate resting on a viscoelastic foundation under hygro-thermo-mechanical loading using a higher-order integral shear deformation theory with a power-law variation in elastic material constituents. They use a sine-shaped function to calculate out-of-plane shear deformation and incorporate the three-parameter viscous foundation model, including the damping coefficient, to study the bending response.

Carrera *et al.* (2008) employed a unified formulation (UF) and principle of virtual displacements (PVD) to analyze the static behavior of FGM plates subjected to transverse mechanical loadings. Their approach allows for a wide range of plate models to be compared, with thickness functions based on Legendre polynomials to incorporate the dependence of material properties in the thickness direction. Results are validated using 3D exact solutions, highlighting the usefulness of their variable kinematic models for analyzing FG plates. Brischetto *et al.* (2008) extended Carrera's Unified Formulation (CUF) to analyze bending response of a simply supported FG rectangular plate under thermo-mechanical loadings. The temperature field is employed using Fourier's law of heat conduction. Further, Brischetto and Carrera (2010) investigated FG plates under bending using the UF and Reissner's mixed variational theorem (RMVT). Carrera *et al.* (2011) evaluated the effect of

thickness stretching in FGM plate/shell structures and found that additional in-plane variables may be meaningless without considering transverse normal strain effects. They used CUF and compared plate/shell theories with constant transverse displacement to those with linear to fourth order expansion in the thickness direction, studying various plate/shell geometries and grading rates for FGMs. Neves *et al.* (2012, 2013) developed a new hyperbolic sine shear deformation theory for analyzing bending and free vibration of functionally graded plates. The theory accounts for through-the-thickness deformations and uses CUF to derive equations of motion and boundary conditions. The authors also used collocation with radial basis functions to interpolate the results.

In recent research, several studies have utilized the CUF to investigate various aspects of FG structures. Filippi *et al.* (2015) employed the 1D CUF to perform static analyses, generating displacement theories that capture variations in mechanical properties through a hierarchical approach. Building upon this framework, Swaminathan *et al.* (2015) provided a comprehensive review of methods used to analyze the static, dynamic, and stability behavior of FGM plates, shedding light on stress, vibration, and buckling characteristics predicted by different theories. Expanding on the capabilities of the CUF, Fazzolari and Carrera (2014b) conducted a thermal stability analysis of FGM isotropic and sandwich plates, incorporating refined quasi-3D plate models within the CUF. Their investigation considered different temperature distributions and examined the effects of various parameters on critical buckling temperatures. Furthermore, Fazzolari and Carrera (2014a) introduced the Hierarchical Trigonometric Ritz Formulation (HTRF), which combined the Ritz minimum energy method with refined Equivalent Single Layer (ESL) and Zig Zag (ZZ) shell models. The HTRF was then applied to study the free vibration analysis of doubly curved FGM shells, deriving governing differential equations and natural boundary conditions.

Building upon the CUF's hierarchical nature, Mashat *et al.* (2014) conducted free-vibrational analyses of FG structures, exploring refined structural theories through the expansion of unknown displacement variables using various functions. Their investigations involved the Finite Element method within the 1D CUF framework, solving governing equations derived in a weak form using the Principle of Virtual Displacements. Their study encompassed various structures, including sandwich beams, laminated beams, thin- and thick-walled boxes, and sandwich cylinders.

Sayyad and Ghugal (2014) used sinusoidal shear and normal deformation theory to investigate bending behaviour of laminated composite plates. However, to the author's knowledge, the effectiveness of the TSDT for evaluating FGM plates has yet to be explored extensively. The semi-analytical method is more analytically and computationally complex than TSDT. Hence, the objective of current study is to analyse bending behaviour of exponentially varied FG plates using TSDT. The effect of transverse normal strain is examined as a novelty. Comprehensive results with various gradation factors for thick, moderately thick, and thin FGM plates are presented. The accuracy of TSDT is verified with semi-analytical solutions generated by authors. Governing equations and boundary conditions are derived using principle of virtutal work. Navier's solution technique is used to solve simply supported plate under bending. The numerical solutions obtained are compared with the semi-analytical solutions to verify the efficacy of the present theory.

2. Theoretical formulation

A linearly elastic and orthotropic FG plate as shown in Fig. 1 of dimensions a and b, with constant thickness h and origin O is considered for the analysis. The top upper surface of the plate (i.e., at $z = -h/z$) is subjected to the transverse mechanical load $q(x, y)$. The plate occupies the

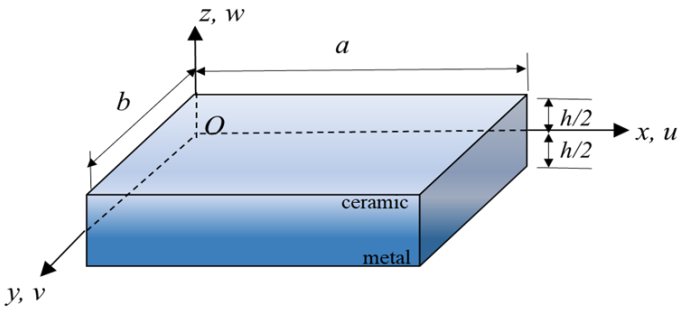

Fig. 1 FG plate under consideration

region in Cartesian coordinates: $0 \le x \le a; 0 \le y \le b;\ -h/2 \le z \le h/2$.

The assumed displacement field of present theory is given as follow

$$\begin{aligned} U &= u_0 - z\ w_{,x} + f(z)\phi(x,y) \\ V &= v_0 - z\ w_{,y} + f(z)\psi(x,y) \\ W &= w(x,y) + g(z)\xi(x,y) \end{aligned} \tag{1}$$

where $f(z) = \frac{h}{\pi}\sin\frac{\pi z}{h}$ and $g(z) = \frac{h}{\pi}\cos\frac{\pi z}{h}$ are the transverse shear and normal strain functions, respectively; u, v, and w are the in-plane displacements and transverse displacement in the x, y and z directions. The extension components u_o and v_o are the displacements at the middle surface which are purely functions of x and y only. Effect of transverse normal strain is considered in displacement field of the theory. Based on the shear stress distribution through the thickness of the plate, trigonometric functions are assigned according to transverse shear stress distribution through the thickness of the plate satisfying the traction free boundary conditions on the top and bottom surfaces of the plate. The unknown functions ϕ, ψ and ξ of position (x,y) that represent the rotations of the normal of a plate at its neutral surface.

The infinitesimally small normal and shear strains within the framework of linear theory of elasticity are given as follows:

Normal strains

$$\begin{aligned} \varepsilon_x &= U_{,x} = u_{0,x} - z\ w_{,xx} + f(z)\phi_{,x} \\ \varepsilon_y &= V_{,y} = v_{0,y} - z\ w_{,yy} + f(z)\psi_{,y} \\ \varepsilon_z &= w_{,x} = -\xi\sin\frac{\pi z}{h} \end{aligned} \tag{2}$$

Shear strains

$$\begin{aligned} \gamma_{xy} &= u_{,y} + v_{,x} = u_{0,y} + v_{0,x} - 2zw_{,xy} + f(z)\left(\phi_{,x} + \psi_{,y}\right) \\ \gamma_{zx} &= u_{,z} + w_{,x} = \cos\frac{\pi z}{h}\left(\frac{h}{\pi}\xi_{,x} + \phi\right) \\ \gamma_{zy} &= v_{,z} + w_{,y} = \cos\frac{\pi z}{h}\left(\frac{h}{\pi}\xi_{,y} + \psi\right) \end{aligned} \tag{3}$$

As the FGM plate is orthotropic at each layer of thickness, hence the stress-strain relationships can be written as

$$\begin{Bmatrix}\sigma_x\\ \sigma_y\\ \sigma_z\\ \tau_{xy}\\ \tau_{yz}\\ \tau_{zx}\end{Bmatrix}=\begin{bmatrix}Q_{11} & Q_{12} & Q_{13} & 0 & 0 & 0\\ Q_{12} & Q_{22} & Q_{23} & 0 & 0 & 0\\ Q_{13} & Q_{23} & Q_{33} & 0 & 0 & 0\\ 0 & 0 & 0 & Q_{66} & 0 & 0\\ 0 & 0 & 0 & 0 & Q_{44} & 0\\ 0 & 0 & 0 & 0 & 0 & Q_{55}\end{bmatrix}\begin{Bmatrix}\varepsilon_x\\ \varepsilon_y\\ \varepsilon_z\\ \gamma_{xy}\\ \gamma_{yz}\\ \gamma_{zx}\end{Bmatrix} \tag{4}$$

where Q_{ij} are the reduced stiffness coefficient as given below

$$\begin{gathered}Q_{11}=Q_{22}=Q_{33}=\frac{E(z)(1-\mu^2)}{\Delta};\\ Q_{12}=\ Q_{13}=Q_{23}=\frac{E(z)(\mu+\mu^2)}{\Delta}.\\ Q_{66}=Q_{55}=Q_{44}=G;\Delta=1-3\mu^2-2\mu^3\end{gathered} \tag{5}$$

where $E(z)$ is the Young's modulus of the material, which is distributed continuously throughout the thickness of a plate according to the exponential law. Which is given by

$$E(z)=E_o e^{\lambda\left(z+\frac{h}{2}\right)} \tag{6}$$

where $\lambda=-ln\frac{E_o}{E_h}$ is the gradation factor, E_h and E_o are the Young's moduli of the FGM plate at top and bottom surfaces respectively, G is the shear modulus and $\mu$is the Poisson's ratio.

2.1 Governing equations and boundary conditions

For the plate, the principle of virtual work can be expressed analytically as follows

$$\int_{dV}\sigma_{ij}\delta\varepsilon_{ij}\ dV-\int_{dA}q(x,y)\delta w\ dA=0,(i,j=x,y,z) \tag{7}$$

where $\sigma_{ij}=\left(\sigma_x,\sigma_y,\sigma_z,\tau_{xy},\tau_{yz},\tau_{xz}\right)^T$
and $\varepsilon_{ij}=\left(\varepsilon_x,\varepsilon_x,\varepsilon_x,\gamma_{xy},\gamma_{yz},\gamma_{xz}\right)^T$ are the stress and strain vectors.

Integrating the Eq. (7) by parts and collecting the coefficients of $\delta u_0,\delta v_0,\delta w_0,\delta\phi,\delta\xi,\delta\psi$ and equating them to zero yields the governing equations and corresponding plate boundary conditions in terms of stress resultants. The governing differential equations are as follows

$$\begin{gathered}N_{x,x}+N_{xy,y}=0\\ N_{xy,x}+N_{y,y}=0\\ M_{x,xx}+2M_{xy,xy}+M_{y,yy}+q(x,y)=0\\ M^s_{x,x}+M^s_{xy,y}-V^s_{xz}=0\\ M^s_{y,y}+M^s_{xy,x}-V^s_{yz}=0\\ V^s_{xz,x}+V^s_{yz,y}-\frac{h}{\pi}V^s_{zz}=0\end{gathered} \tag{8}$$

It is necessary to prescribe one of each of the following 14 products along the edges of the plate to meet the boundary conditions.

$$\begin{gathered}N_x u_0,N_{xy}v_0,V_x w,M_x w_{,x},M^s_x\phi,M^s_{xy}\psi,V^s_{xz}\xi\quad\text{for } x=0 \text{ and } x=a\\ N_{xy}u_0,N_y v_0,V_y w,M_y w_{,y},M^s_{xy}\phi,M^s_y\psi,V^s_{yz}\xi\quad\text{for } y=0 \text{ and } y=b\end{gathered} \tag{9}$$

where $V_x=M_{x,x}+2M_{xy,y}$ and $V_y=M_{y,y}+2M_{xy,x}$

At the corners, the boundary condition is:

Either $M_{xy} = 0$ or w is prescribed

The force and the moment resultants in the governing equations and the boundary conditions are defined as follows

$$\begin{pmatrix} N_x & M_x & M_x^s \\ N_y & M_y & M_y^s \\ N_{xy} & M_{xy} & M_{xy}^s \end{pmatrix} = \int_{\frac{-h}{2}}^{\frac{h}{2}} \begin{Bmatrix} \sigma_x \\ \sigma_y \\ \sigma_{xy} \end{Bmatrix} \big(1 z f(z)\big) dz$$

$$\begin{bmatrix} V_{xz}^s \\ V_{yz}^s \end{bmatrix} = \int_{\frac{-h}{2}}^{\frac{h}{2}} \begin{Bmatrix} \tau_{xz} \\ \tau_{yz} \end{Bmatrix} \left(\cos\frac{\pi z}{h}\right) dz, \tag{10}$$

$$V_{zz}^s = -\int_{\frac{-h}{2}}^{\frac{h}{2}} \sigma_{zz} \sin\frac{\pi z}{h}\, dz.$$

where in-plane stress resultants $\left(N_x, N_y, N_{xy}\right)$ and moment resultants $\left(M_x, M_y, M_{xy}\right)$ are analogous to CPT. $\left(M_x^s, M_y^s, M_{xy}^s\right)$ are moments due to transverse shear deformation effect and $\left(V_{xz}^s, V_{yz}^s, V_{zz}^s\right)$ are the shear force resultants.

The governing equations in terms of displacement variables can be expressed for static analysis as follows

$$\begin{gathered}
\delta u_0: -A_{11}u_{0,xx} - A_{66}u_{0,yy} - (A_{12} + A_{66})v_{0,xy} + B_{11}w_{,xxx} + (B_{12} + 2B_{66})w_{,xyy} - \\
As_{11}\phi_{,xx} - As_{66}\phi_{,yy} - (As_{12} + As_{66})\psi_{,xy} + As_{13}\frac{\pi}{h}\xi_{,x} = 0 \\
\delta v_0: -(A_{12} + A_{66})u_{0,xy} - A_{66}v_{0,xx} - A_{22}v_{0,yy} + B_{22}w_{,yyy} + (B_{12} + 2B_{66})w_{,xxy} - (As_{66} + \\
As_{12})\phi_{,xy} - As_{66}\psi_{,xx} - As_{22}\psi_{,yy} + As_{23}\frac{\pi}{h}\xi_{,y} = 0 \\
\delta w: -B_{11}u_{0,xxx} - (B_{12} + 2B_{66})\big(u_{0,xyy} + v_{0,xxy}\big) - B_{22}v_{0,yyy} + D_{11}w_{,xxxx} + D_{22}w_{,yyyy} - \\
Bs_{11}\phi_{,xxx} + (2D_{12} + 4D_{66})w_{,xxyy} - Bs_{22}\psi_{,yyy} - (Bs_{12} + 2Bs_{66})\big(\phi_{,xyy} + \psi_{,xxy}\big) + \\
Bs_{13}\frac{\pi}{h}\xi_{,xx} + Bs_{23}\frac{\pi}{h}\xi_{,yy} = q(x,y) \\
\delta\phi: -As_{11}u_{0,xx} - As_{66}u_{0,yy} - (As_{12} + As_{66})v_{0,xy} + Bs_{11}w_{,xxx} + (Bs_{12} + 2Bs_{66})w_{,xyy} - \\
Ass_{11}\phi_{,xx} - Ass_{66}\phi_{,yy} + Acc_{55}\phi - (Ass_{12} + Ass_{66})\psi_{,xy} + As_{13}\frac{\pi}{h}\xi_{,x} + Acc_{55}\frac{\pi}{h}\xi_{,x} = 0 \\
\delta\psi: -(As_{12} + As_{66})u_{0,xy} - As_{66}v_{0,xx} - As_{22}v_{0,yy} + Bs_{22}w_{,yyy} + (Bs_{12} + 2Bs_{66})w_{,xxy} - \\
Ass_{66}\psi_{,xx} - Ass_{22}\psi_{,yy} + Acc_{44}\psi - (Ass_{12} + Ass_{66})\phi_{,xy} - Ass_{23}\frac{\pi}{h}\xi_{,y} + Acc_{44}\frac{h}{\pi}\xi_{,y} = 0 \\
\delta\xi: -\frac{\pi}{h}As_{13}u_{0,x} - \frac{\pi}{h}As_{23}v_{0,y} + \frac{\pi}{h}Bs_{13}w_{,xx} + \frac{\pi}{h}Bs_{23}w_{,yy} - \frac{\pi}{h}Ass_{13}\phi_{,x} - \frac{h}{\pi}Acc_{55}\phi_{,x} - \\
\frac{\pi}{h}Ass_{23}\psi_{,y} - \frac{h}{\pi}Acc_{44}\psi_{,y} - \frac{h^2}{\pi^2}Acc_{44}\xi_{,yy} - \frac{h^2}{\pi^2}Acc_{55}\xi_{,yy} - Ass_{33}\frac{\pi^2}{h^2}\xi = 0
\end{gathered} \tag{12}$$

where $A_{ij}, B_{ij}, D_{ij}, As_{ij}, B_{ij}, Ass_{ij}, Acc_{ij}$ are the plate stiffnesses defined as follows

$$\left(A_{ij}, B_{ij}, D_{ij}\right) = \int_{\frac{-h}{2}}^{\frac{h}{2}} Q_{ij}\,(1, z, z^2) dz (i, j = 1,2,6)$$

$$\left(As_{ij}, Bs_{ij}\right) = \int_{\frac{-h}{2}}^{\frac{h}{2}} Q_{ij}\, f(z)(1, z) dz (i, j = 1,2,3,6)$$

$$Ass_{ij} = \int_{-\frac{h}{2}}^{\frac{h}{2}} Q_{ij} f(z)^2 dz\,(i, j = 1,2,3,6)$$

$$Acc_{ij} = \int_{-\frac{h}{2}}^{\frac{h}{2}} Q_{ij} \cos^2 \frac{\pi z}{h} dz \; (i,j = 4,5) \tag{13}$$

3. Navier's solutions

A Navier's solution is developed in this section for a simply supported rectangular plate that meets the following boundary conditions.

at $x = 0$ and $x = a$.

$$N_x = v_0 = w = \psi = \xi = M_x^b = M_x^s = 0 \tag{14}$$

at $y = 0$ and $y = b$.

$$N_y = u_0 = w = \psi = \xi = M_y^b = M_y^s = 0 \tag{15}$$

In double Fourier series, the applied load $q(x, y)$ can be expanded as follows:

$$q(x,y) = \sum_{m=1}^{\infty} \sum_{n=1}^{\infty} q_{mn} \sin \alpha x \sin \beta y \tag{16}$$

where $\alpha = \frac{m\pi}{a}$ and $\beta = \frac{n\pi}{b}$. q_{mn} are the coefficients of Fourier series expansion. $q_{mn} = q_o$ for the bi-sinusoidally distributed load (SDL) and $q_{mn} = \frac{16q_0}{mn\pi^2}$ for uniformly distributed load (UDL). q_o is the load intensity at the plate center and *m*, *n* are the integers. The unknown variables, which exactly satisfy governing Eq. (12) and boundary conditions, Eqs. (14)-(15) exactly are presented in double trigonometric series as follows

$$\begin{Bmatrix} u_0 \\ v_0 \\ w \\ \phi \\ \psi \\ \xi \end{Bmatrix} = \sum_{m=1}^{\infty} \sum_{n=1}^{\infty} \begin{Bmatrix} u_{mn} \cos \alpha \, \mathrm{x} \sin \beta \, \mathrm{y} \\ v_{mn} \sin \alpha \, \mathrm{x} \cos \beta \, \mathrm{y} \\ w_{mn} \sin \alpha \, \mathrm{x} \sin \beta \, \mathrm{y} \\ \phi_{mn} \cos \alpha \, \mathrm{x} \sin \beta \, \mathrm{y} \\ \psi_{mn} \sin \alpha \, \mathrm{x} \cos \beta \, \mathrm{y} \\ \xi_{mn} \sin \alpha \, \mathrm{x} \sin \beta \, \mathrm{y} \end{Bmatrix} \tag{17}$$

where $u_{mn}, v_{mn}, w_{mn}, \phi_{mn}, \psi_{mn}$, and ξ_{mn} are the unknown coefficients of respective Fourier expansion. Substitution of Eqs. (16) and (17) into Eq. (12) yields system of algebraic equations which can be written in matrix form as follows

$$\{F\} = [K]\{\Delta\} \tag{18}$$

where

$$[K] = \begin{bmatrix} K_{11} & K_{12} & K_{13} & K_{14} & K_{15} & K_{16} \\ K_{12} & K_{22} & K_{23} & K_{24} & K_{25} & K_{26} \\ K_{13} & K_{23} & K_{33} & K_{34} & K_{35} & K_{36} \\ K_{14} & K_{24} & K_{34} & K_{44} & K_{45} & K_{46} \\ K_{15} & K_{25} & K_{35} & K_{45} & K_{55} & K_{56} \\ K_{16} & K_{26} & K_{36} & K_{46} & K_{56} & K_{66} \end{bmatrix} \text{ where } K_{ij} = K_{ji},$$

$$\{\Delta\} = \begin{Bmatrix} u_{mn} \\ v_{mn} \\ w_{mn} \\ \phi_{mn} \\ \psi_{mn} \\ \xi_{mn} \end{Bmatrix} \text{ and } \{F\} = \begin{Bmatrix} 0 \\ 0 \\ q_{mn} \\ 0 \\ 0 \\ 0 \end{Bmatrix} \tag{19}$$

The elements of the stiffness matrix $[K]$ are defined in the Appendix. Solving Eq. (18), the unknown series coefficients $u_{mn}, v_{mn}, w_{mn}, \phi_{mn}, \psi_{mn}$, and ξ_{mn} are obtained. Using these coefficients, one can obtained displacements and stresses within the plate using following expressions.

$$U = \begin{Bmatrix} u_{mn} - \left(\frac{z}{h}\right) h\alpha w_{mn} \\ +\frac{h}{\pi}\sin\frac{\pi z}{h}\phi_{mn} \end{Bmatrix} \cos\alpha\, x \sin\beta\, y \tag{20}$$

$$V = \begin{Bmatrix} v_{mn} - \left(\frac{z}{h}\right) h\beta w_{mn} \\ +\frac{h}{\pi}\sin\frac{\pi z}{h}\psi_{mn} \end{Bmatrix} \sin\alpha\, x \cos\beta\, y \tag{21}$$

$$W = \left\{w_{mn} + \left(\frac{h}{\pi}\right)\cos\frac{\pi z}{h}\xi_{mn}\right\} \sin\alpha\, x \sin\alpha\, y \tag{22}$$

$$\sigma_x = \begin{Bmatrix} Q_{11}\begin{bmatrix} -\alpha u_{mn} + \left(\frac{z}{h}\right) h\alpha^2 w_{mn} \\ -\frac{h}{\pi}\sin\frac{\pi z}{h}\alpha\phi_{mn} \end{bmatrix} \\ +Q_{12}\begin{bmatrix} -\beta v_{mn} + \left(\frac{z}{h}\right) h\beta^2 w_{mn} \\ -\frac{h}{\pi}\sin\frac{\pi z}{h}\beta\psi_{mn} \end{bmatrix} \\ -Q_{13}\sin\frac{\pi z}{h}\xi_{mn} \end{Bmatrix} \sin\alpha\, x \sin\beta\, y \tag{23}$$

$$\sigma_y = \begin{Bmatrix} Q_{12}\begin{bmatrix} -\alpha u_{mn} + \left(\frac{z}{h}\right) h\alpha^2 w_{mn} \\ -\frac{h}{\pi}\sin\frac{\pi z}{h}\alpha\phi_{mn} \end{bmatrix} + \\ Q_{22}\begin{bmatrix} -\beta v_{mn} + \left(\frac{z}{h}\right) h\beta^2 w_{mn} \\ -\frac{h}{\pi}\sin\frac{\pi z}{h}\beta\psi_{mn} \end{bmatrix} \\ -Q_{23}\sin\frac{\pi z}{h}\xi_{mn} \end{Bmatrix} \sin\alpha\, x \sin\beta\, y \tag{24}$$

$$\tau_{xy} = Q_{66}\begin{Bmatrix} \beta u_{mn} + \alpha v_{mn} \\ -2\left(\frac{z}{h}\right) h\alpha\beta w_{mn} \\ +\frac{h}{\pi}\sin\frac{\pi z}{h}[\beta\phi_{mn} + \alpha\psi_{mn}] \end{Bmatrix} \cos\alpha\, x \cos\beta\, y \tag{25}$$

The use of constitutive relations gives less accurate results of transverse shear stresses. Hence, these stresses are recovered by integrating the equations of stress equilibrium through the thickness of the FG plate. These equations are defined as follows:

Table 1 Normalized displacements $(\bar{u}, \bar{w})$ and stresses $\left(\bar{\sigma}_x, \bar{\sigma}_y, \bar{\tau}_{xy}, \bar{\tau}_{xz}, \bar{\tau}_{yz}\right)$ for FG square plate of material I subjected to sinusoidal load

S	Source	$\bar{u}$	$\bar{w}$	$\bar{\sigma}_x$	$\bar{\tau}_{xy}$	$\bar{\tau}_{xz}$(max)
5	Ref.*	-0.0564	4.9165	0.2702	0.0832	0.2393
	TSDT	-0.0576	4.7535	0.2847	0.0796	0.2387
	TSDT*	-0.0488	4.2866	0.2949	0.0698	0.2378
	CPT	-0.0463	3.3763	0.2798	0.067	0.2407
10	Ref.*	-0.0566	4.3202	0.2583	0.0824	0.24035
	TSDT	-0.0575	4.2495	0.2731	0.0795	0.2390
	TSDT*	-0.0469	3.6046	0.2836	0.0677	0.2400
	CPT	-0.0463	3.3763	0.2798	0.067	0.2407
20	Ref.*	-0.0567	4.1814	0.2555	0.0821	0.24062
	TSDT	-0.0575	4.1275	0.2703	0.0795	0.2383
	TSDT*	-0.0465	3.4335	0.2807	0.0671	0.2405
	CPT	-0.0463	3.3763	0.2798	0.067	0.2407
50	Ref.*	-0.0567	4.1433	0.2547	0.0820	0.2407
	TSDT	-0.0575	4.0936	0.2695	0.0794	0.2385
	TSDT*	-0.0463	3.3855	0.2799	0.067	0.2407
	CPT	-0.0463	3.3763	0.2798	0.067	0.2407

Ref.*= Pendhari *et al.* (2012)

$$\tau_{xz} = -\int\left(\sigma_{x,x} + \tau_{xy,y}\right)dz + C_1,\ \tau_{yz} = -\int\left(\sigma_{y,y} + \tau_{xy,x}\right)dz + C_2$$

4. Numerical results and discussion

Based on the trigonometric shear deformation theory with and without transverse normal deformation a computer programme in MATLAB is developed to analyse the bending response of exponentially varying FG plates subjected to transverse loads. Numerical investigations with different aspect ratios '*S*' of simply supported square and rectangular plates have been performed. The material properties of the FG plate for material I vary exponentially between Aluminium at bottom surface and Zirconia at top surface of the plate. Also, for material II, the material properties follow the exponential law of distribution throughout the thickness of the plate, where results are obtained with various gradation factors. The body forces are neglected for the sake of simplicity. Results of numerical investigations are obtained using the following normalizations:

$$\bar{w} = \frac{100E_h h^3}{q_o a^4} w\left(\frac{a}{2}, \frac{b}{2}, z\right), \bar{u} = \frac{E_h}{q_o h a^3} u\left(0, \frac{b}{2}, z\right),$$
$$\bar{v} = \frac{E_h}{q_o h a^3} v\left(\frac{a}{2}, 0, z\right), \bar{\sigma}_{xx} = \frac{h}{q_o a^2}\sigma_{xx}\left(\frac{a}{2}, \frac{b}{2}, z\right),$$
$$\bar{\sigma}_{yy} = \frac{h}{q_o a^2}\sigma_{yy}\left(\frac{a}{2}, \frac{b}{2}, z\right), \bar{\tau}_{xy} = \frac{h}{q_o a^2}\tau_{xy}(0,0,z)$$
$$\bar{\tau}_{xz} = \frac{h}{q_o a}\tau_{xz}\left(0, \frac{b}{2}, z\right), \bar{\tau}_{yz} = \frac{h}{q_o a}\tau_{yz}\left(\frac{a}{2}, 0, z\right),$$
$$E_r = \frac{E_h}{E_0} \text{ and } S = a/h.$$

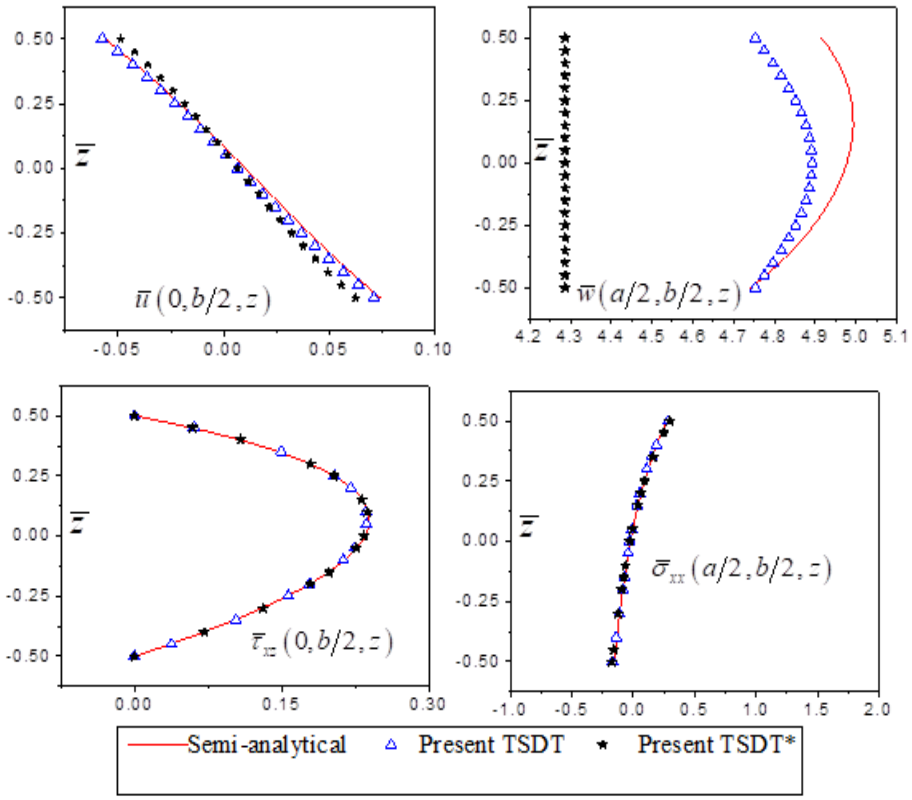

Fig. 2 Through thickness variation of displacements $(\bar{u}\ ,\bar{w})$, in-plane normal stress $(\bar{\sigma}_{xx})$, and transverse shear stresses $(\bar{\tau}_{xz})$ for sinusoidal loading in FG square plate $(a/h = 5)$ of Material I

The material properties used in the analysis are as below:

Material I : Praveen and Reddy (1998): E_o= 70 GPa (Aluminium), E_h= 151 GPa (Zirconia) and μ=0.3

Material II : Pendhari *et al.* (2012): E_o= 1 GPa, E_r=5, 10, 20, 30 and 40

The results of the present theory are compared with those of CPT, the trigonometric shear deformation theory with $(\varepsilon_z \neq 0)$ TSDT and without transverse normal deformation $(\varepsilon_z = 0)$ TSDT* and the semi-analytical solution obtained by Pendhari *et al.* (2012). Numerical results of displacements and stresses for different aspect ratios 5, 10, 20 and 50 with various values of E_r ratio are presented numerically and graphically.

Example 1.

A simply supported square FG plate made up of material I is subjected to sinusoidal load. The comparison of results of TSDT with the semi-analytical and CPT is presented. The normalized in-plane displacement $(\bar{u})$ and the transverse displacement $(\bar{w})$, in-plane normal stresses $(\bar{\sigma}_{xx})$, transverse shear stress $(\bar{\tau}_{xz})$, for the aspect ratios (S) 5,10,20 and 50 are presented in Table 1. The through-thickness variations of in-plane and transverse displacement $(\bar{u},\bar{w})$ as well as transverse shear stresses $(\bar{\tau}_{xz})$ and in-plane normal stress $(\bar{\sigma}_{xx})$ for S=5, are shown in Fig. 2. The through thickness variation of in-plane and transverse displacement $(\bar{u},\bar{w})$ are in good agreement with semi-

Table 2 Normalized displacements $(\bar{u}, \bar{v}, \bar{w})$ and stresses $\left(\bar{\sigma}_x, \bar{\sigma}_y, \bar{\tau}_{xy}, \bar{\tau}_{xz}, \bar{\tau}_{yz}\right)$ of rectangular FG plate under sinusoidal load for material I

S	Source	$\overline{u}$	$\overline{v}$	$\overline{w}$	$\bar{\sigma}_x$	$\bar{\sigma}_y$	$\bar{\tau}_{xy}$	$\bar{\tau}_{xz}$(max)	$\bar{\tau}_{yz}$(max)
5	Ref.*	-0.1445	-0.0722	11.8020	0.5535	0.2916	0.1060	0.3837	0.1919
	TSDT	-0.1472	-0.0736	11.5157	0.5796	0.3127	0.1017	0.3793	0.1916
	TSDT*	-0.1226	-0.0613	10.1021	0.5739	0.3517	0.088	0.3822	0.1911
	CPT	-0.1185	-0.0593	8.6435	0.555	0.3402	0.0857	0.3851	0.1926
10	Ref.*	-0.1450	-0.0725	10.8808	0.5424	0.2796	0.1053	0.3848	0.1924
	TSDT	-0.1472	-0.0736	10.7221	0.5681	0.3014	0.1017	0.3809	0.1914
	TSDT*	-0.1196	-0.0598	9.0088	0.5598	0.3431	0.0863	0.3844	0.1922
	CPT	-0.1185	-0.0593	8.6435	0.555	0.3402	0.0857	0.3851	0.1926
20	Ref.*	-0.1452	-0.0726	10.6608	0.5398	0.2767	0.1051	0.3851	0.1925
	TSDT	-0.1471	-0.0736	10.5277	0.5653	0.2986	0.1017	0.3813	0.1909
	TSDT*	-0.1188	-0.0594	8.7348	0.5562	0.3409	0.0858	0.385	0.1925
	CPT	-0.1185	-0.0593	8.6435	0.555	0.3402	0.0857	0.3851	0.1926
50	Ref.*	-0.1452	-0.0726	10.5999	0.5391	0.2759	0.1050	0.3851	0.1926
	TSDT	-0.1471	-0.0736	10.4735	0.5645	0.2978	0.1017	0.3814	0.1908
	TSDT*	-0.1186	-0.0593	8.6581	0.5552	0.3403	0.0857	0.3851	0.1926
	CPT	-0.1185	-0.0593	8.6435	0.555	0.3402	0.0857	0.3851	0.1926

Ref.*= Pendhari *et al.* (2012)

analytical results. The in-plane displacement shows non-linear variation across the thickness of FG plate. The maximum value of this displacement is observed at bottom face of the plate and minimum at the top face. In TSDT with transverse normal deformation effect, the transverse displacement across the thickness varies according to cosine law and is almost symmetric about the midplane of the FG plate. The through thickness variation of in-plane and transverse stresses $(\bar{\sigma}_{xx}, \bar{\tau}_{xz})$ using TSDT are exactly matching with semi-analytical solutions.

The through thickness variations of in-plane displacements obtained by TSDT with transverse normal effect are in excellent agreement with variations given by semi-analytical, whereas TSDT without transverse effect deviates slightly from the semi-analytical theory. TSDT without transverse normal strain shows considerable departure in transverse displacements from the TSDT and semi-analytical solutions, whereas TSDT with transverse normal effect and semi-analytical theory are in close agreement at top surface of plate. The through thickness distribution of in-plane normal stress $(\bar{\sigma}_{xx})$ obtained using TSDT with and without transverse normal stress is in excellent agreement with that is given by semi-analytical method. However, in-plane normal stress $\left(\bar{\sigma}_{yy}\right)$ shows marginal deviations at top face of plate. The transverse shear stresses and their variations are in close agreement with those given by semi-analytical solutions as seen from Table 2 and Fig. 3.

Example 2.

In this example, a simply supported rectangular FG plate made of material I is subjected to sinusoidal load. The comparison of results of TSDT with the semi-analytical method and CPT is presented. The normalized displacements and stresses for the aspect ratios (S) 5, 10, 20 and 50 are represented in Table 2. The through-thickness distributions of displacements and stresses for S=5, are shown in Fig. 3.

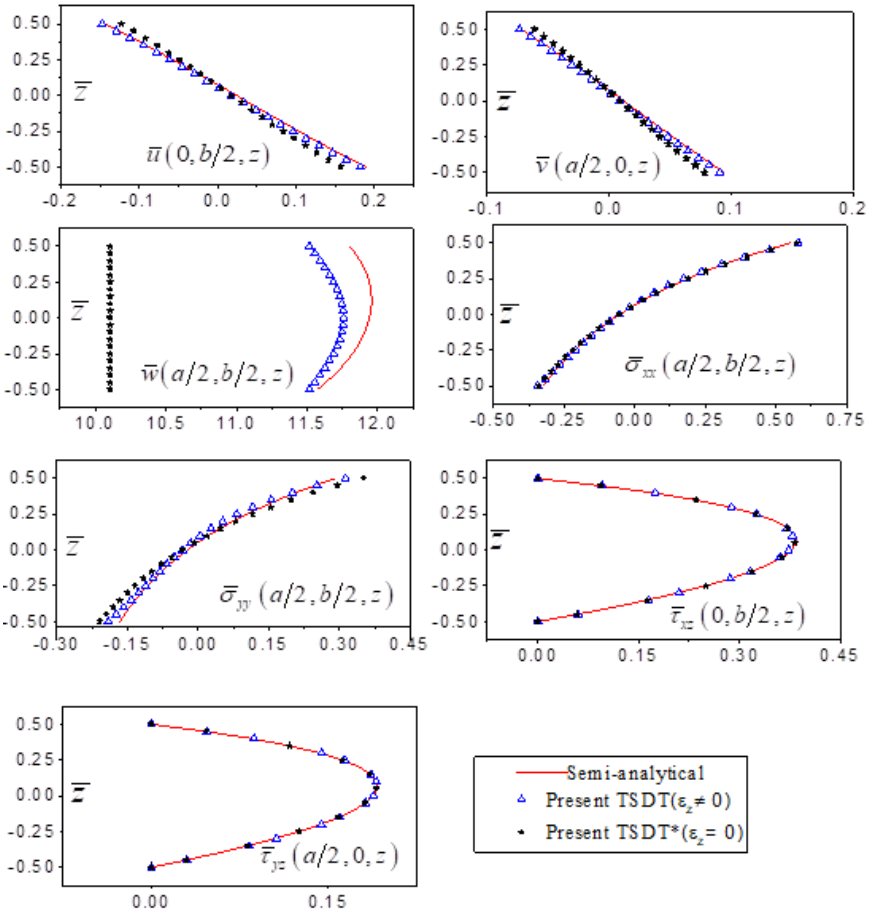

Fig. 3 Through thickness distribution of non-dimensional in-plane displacement and transverse displacement ($\bar{u}$, $\bar{w}$), in-plane normal stresses $(\bar{\sigma}_{xx}, \bar{\sigma}_{yy})$, and transverse shear stresses $(\bar{\tau}_{xz}, \bar{\tau}_{yz})$ for sinusoidal loading in FG rectangular plate $(a/h = 5)$ and $(b/a = 2)$ for Material I

Table 3 Normalized displacements $(\bar{u}, \bar{v}, \bar{w})$ and stresses $(\bar{\sigma}_x, \bar{\sigma}_y, \bar{\tau}_{xy}, \bar{\tau}_{xz}, \bar{\tau}_{yz})$ of square FG plate subjected to UDL for different gradation factors for material II

S	E_r	$\bar{u}$				$\bar{w}$			
		Ref.*	TSDT	TSDT*	CPT	Ref.*	TSDT	TSDT*	CPT
5	5	-0.127	-0.1276	-0.1088	-0.1017	11.859	11.4654	10.1762	8.254
	10	-0.1606	-0.1584	-0.1361	-0.1271	16.966	15.9187	14.3941	11.849
	20	-0.202	-0.1949	-0.1697	-0.1585	24.129	21.9978	20.2739	16.985
	40	-0.2525	-0.2382	-0.2105	-0.1971	34.007	30.2303	28.3482	24.195
10	5	-0.125	-0.1266	-0.1035	-0.1017	10.536	10.1736	8.7354	8.2536
	10	-0.1568	-0.1567	-0.1294	-0.1271	15.116	14.1862	12.4876	11.849
	20	-0.196	-0.1924	-0.1613	-0.1585	21.626	19.7268	17.8099	16.985
	40	-0.2442	-0.2346	-0.2005	-0.1971	30.721	27.3243	25.2372	24.195
50	5	-0.1246	-0.1264	-0.1018	-0.1017	10.127	9.7567	8.2729	8.2536
	10	-0.1557	-0.1563	-0.1272	-0.1271	14.54	13.6271	11.8753	11.849
	20	-0.1942	-0.1917	-0.1586	-0.1585	20.839	18.994	17.0183	16.985
	40	-0.2415	-0.2336	-0.1972	-0.1971	29.6829	26.3866	24.2374	24.195

Table 3 Continued

S	E_r	$\bar{\sigma}_{xx}$				$\bar{\tau}_{xy}$				$\bar{\tau}_{xz}$			
		Ref.*	TSDT	TSDT*	CPT	Ref.*	TSDT	TSDT*	CPT	Ref.*	TSDT	TSDT*	CPT
5	5	0.5091	0.5379	0.5576	0.5348	0.1102	0.1063	0.0972	0.0909	0.5061	0.4897	0.4916	0.5039
	10	0.6365	0.6729	0.6974	0.6682	0.0839	0.0794	0.0741	0.0703	0.5366	0.5247	0.5222	0.5241
	20	0.7938	0.8400	0.8694	0.8333	0.0629	0.0586	0.0556	0.0535	0.5763	0.5660	0.562	0.553
	40	0.9863	1.0454	1.0796	1.0362	0.0463	0.0426	0.0411	0.0400	0.6218	0.6153	0.6071	0.5908
10	5	0.4921	0.5198	0.5406	0.5348	0.1114	0.1042	0.0926	0.0909	0.5092	0.4985	0.5005	0.5039
	10	0.6151	0.6498	0.6756	0.6682	0.0857	0.0781	0.0713	0.0703	0.5331	0.5233	0.5235	0.5241
	20	0.7670	0.8113	0.8425	0.8333	0.0649	0.0579	0.0541	0.0535	0.5641	0.5550	0.5535	0.5530
	40	0.9536	1.0108	1.0473	1.0362	0.0482	0.0423	0.0403	0.0400	0.6043	0.5947	0.5936	0.5908
50	5	0.4867	0.5140	0.5350	0.5348	0.1115	0.1039	0.0910	0.0909	0.5086	0.5016	0.5037	0.5039
	10	0.6082	0.6423	0.6685	0.6682	0.0862	0.0779	0.0703	0.0703	0.5291	0.5238	0.5240	0.5241
	20	0.7584	0.8021	0.8337	0.8333	0.0656	0.0578	0.0535	0.0535	0.5583	0.5525	0.5529	0.553
	40	0.9431	0.9996	1.0367	1.0362	0.0490	0.0423	0.0400	0.0400	0.5967	0.5921	0.5909	0.5908

Ref.*= Pendhari *et al.* (2012)

Example 3

A simply supported square FG plate made up of material II is subjected to uniformly distributed load. The comparison of results of TSDT with the semi-analytical method and CPT is presented. The normalized in-plane displacement ($\bar{u}$) and the transverse displacement ($\bar{w}$), in-plane normal stress ($\bar{\sigma}_{xx}$), transverse shear stress ($\bar{\tau}_{xz}$), for the aspect ratios 5,10 and 50 and various E_h/E_0 ratios are presented in Table 3. The through-thickness variations of as in-plane and transverse displacements ($\bar{u}, \bar{w}$) and in-plane normal stress ($\bar{\sigma}_{xx}$), and transverse shear stress ($\bar{\tau}_{xz}$) for an aspect ratio 5 and $E_h/E_0 = 10$ are shown in Fig. 4

Results in Table 3 indicate that the maximum value of in-plane displacement ($\bar{u}$) obtained using TSDT ($\varepsilon_z \neq 0$) at bottom face of plate is matches excellently with the one given by semi-analytical solutions. The variation of in-plane displacement ($\bar{u}$) is closely matching with the one given by semi-analytical solution in the lower half of plate, whereas, little departure in upper half of the plate. The through thickness variation of in-plane and transverse stresses ($\bar{\sigma}_{xx}, \bar{\tau}_{xz}$) using TSDT are exactly matching with semi-analytical solutions.

The through thickness variation of in-plane and transverse displacement ($\bar{u}, \bar{w}$) are in good agreement with semi-analytical results. The in-plane displacement shows non-linear variation across the thickness of FG plate.

The maximum value of this displacement is observed at bottom face of the plate and minimum at the top face. In TSDT with transverse normal deformation effect, the transverse displacement across the thickness varies according to cosine law and is almost symmetric about the mid-plane of the FG plate. The through thickness variation of in-plane and transverse stresses ($\bar{\sigma}_{xx}, \bar{\tau}_{xz}$) using TSDT are exactly matching with semi-analytical solutions

Example 4

In this example, a simply supported rectangular FG plate made of material II is subjected to uniformly distributed load. The normalized displacements and stresses for the *S*=5, 10 and 50 are represented in Table 4. The through-thickness variations of displacements and stresses for *S*=5, are

shown in Fig. 5. The normalized in-plane and transverse displacements $(\bar{u}, \bar{v}, \bar{w})$, in-plane stresses $(\bar{\sigma}_{xx}, \bar{\sigma}_{yy}, \bar{\tau}_{xy})$, and transverse shear stresses $(\bar{\tau}_{xz}, \bar{\tau}_{yz})$ for the aspect ratios 5, 10 and 50 and E_h/E_0=5, 10, 20, 30 and 40 are represented in Table 4.

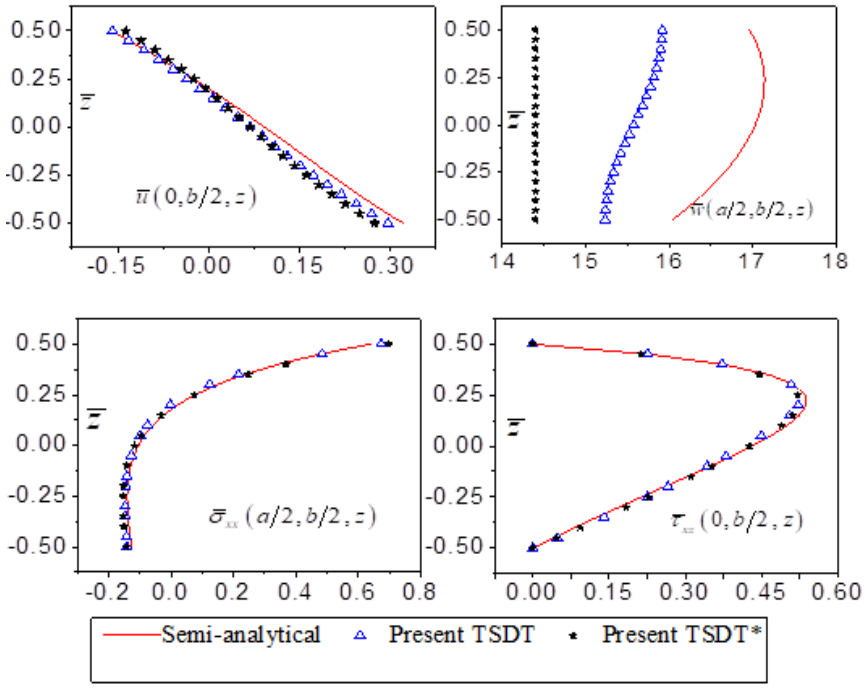

Fig. 4 Variation of normalized in-plane displacement $(\bar{u})$, transverse displacement $(\bar{w})$, in-plane normal stresses $(\bar{\sigma}_{xx})$, in-plane and transverse shear stresses $(\bar{\tau}_{xy}, \bar{\tau}_{xz})$for uniformly distributed loading condition in FG square plate $(a/h = 5)$and E_h/E_0=10 for material II

Table 4 Normalized displacements $(\bar{u}, \bar{v}, \bar{w})$ and stresses $(\bar{\sigma}_{xx}, \bar{\sigma}_{yy}, \bar{\tau}_{xy}, \bar{\tau}_{xz}, \bar{\tau}_{yz})$ of rectangular FG plate subjected to UDL for different gradation factors and material II

S	E_r	$\bar{u}$				$\bar{v}$				$\bar{w}$			
		Ref.*	TSDT	TSDT*	CPT	Ref.*	TSDT	TSDT*	CPT	Ref.*	TSDT	TSDT*	CPT
5	5	-0.304	-0.307	-0.255	-0.246	-0.185	-0.186	-0.156	-0.148	27.878	26.96	23.555	20.579
	10	-0.383	-0.38	-0.320	-0.307	-0.233	-0.231	-0.195	-0.186	39.945	37.509	33.485	29.545
	20	-0.48	-0.468	-0.399	-0.383	-0.293	-0.284	-0.243	-0.232	56.980	51.988	47.442	42.35
	40	-0.599	-0.571	-0.495	-0.476	-0.365	-0.347	-0.303	-0.288	80.623	71.715	66.758	60.327
10	5	-0.302	-0.306	-0.248	-0.246	-0.183	-0.185	-0.151	-0.148	25.864	24.956	21.324	20.579
	10	-0.378	-0.378	-0.310	-0.307	-0.229	-0.229	-0.188	-0.186	37.119	34.82	30.532	29.545
	20	-0.472	-0.464	-0.387	-0.383	-0.286	-0.281	-0.235	-0.232	53.142	48.463	43.626	42.35
	40	-0.587	-0.566	-0.481	-0.476	-0.356	-0.343	-0.292	-0.288	75.571	67.205	61.939	60.327
50	5	-0.301	-0.306	-0.246	-0.246	-0.182	-0.185	-0.149	-0.148	25.235	24.31	20.609	20.579
	10	-0.376	-0.378	-0.307	-0.307	-0.228	-0.229	-0.186	-0.186	36.230	33.955	29.585	29.545
	20	-0.469	-0.463	-0.383	-0.383	-0.284	-0.281	-0.232	-0.232	51.929	47.329	42.401	42.35
	40	-0.584	-0.565	-0.476	-0.476	-0.354	-0.342	-0.288	-0.288	73.967	65.754	60.392	60.327

Table 4 Continued

S	E_r	$\bar{\sigma}_{xx}$				$\bar{\sigma}_{yy}$				$\bar{\tau}_{xy}$			
		Ref.*	TSDT	TSDT*	CPT	Ref.*	TSDT	TSDT*	CPT	Ref.*	TSDT	TSDT*	CPT
5	5	1.057	1.104	1.0858	1.0561	0.493	0.533	0.6141	0.5977	Ref.*	TSDT	TSDT*	CPT
	10	1.323	1.377	1.3575	1.3196	0.614	0.670	0.7678	0.7469	0.158	0.149	0.1351	0.1292
	20	1.652	1.713	1.6926	1.6456	0.763	0.844	0.9574	0.9314	0.121	0.112	0.1035	0.0998
	40	2.055	2.122	2.1028	2.0463	0.947	1.061	1.1894	1.1582	0.091	0.083	0.078	0.076
10	5	1.039	1.085	1.0636	1.0561	0.476	0.516	0.6019	0.5977	0.067	0.060	0.0578	0.0568
	10	1.299	1.353	1.3292	1.3196	0.595	0.648	0.7522	0.7469	0.159	0.148	0.1307	0.1292
	20	1.62	1.682	1.6575	1.6456	0.742	0.817	0.938	0.9314	0.122	0.111	0.1008	0.0998
	40	2.015	2.084	2.0606	2.0463	0.922	1.029	1.1661	1.1582	0.093	0.082	0.0765	0.076
50	5	1.033	1.08	1.0564	1.0561	0.471	0.51	0.5979	0.5977	0.069	0.06	0.0571	0.0568
	10	1.291	1.345	1.32	1.3196	0.589	0.64	0.7471	0.7469	0.159	0.148	0.1292	0.1292
	20	1.61	1.672	1.6461	1.6456	0.735	0.808	0.9317	0.9314	0.123	0.111	0.0999	0.0998
	40	2.002	2.072	2.0469	2.0463	0.913	1.019	1.1585	1.1582	0.093	0.082	0.076	0.076

S	E_r	$\bar{\tau}_{xz}(\max)$				$\bar{\tau}_{yz}(\max)$			
		Ref.*	TSDT	TSDT*	CPT	Ref.*	TSDT	TSDT*	CPT
5	5	0.701	0.684	0.6912	0.7036	0.542	0.522	0.524	0.531
	10	0.744	0.729	0.7299	0.7318	0.571	0.551	0.551	0.552
	20	0.794	0.785	0.7802	0.7721	0.608	0.588	0.586	0.583
	40	0.851	0.846	0.8367	0.8249	0.65	0.629	0.628	0.623
10	5	0.708	0.697	0.7002	0.7036	0.541	0.527	0.529	0.531
	10	0.74	0.731	0.7313	0.7318	0.565	0.552	0.552	0.552
	20	0.782	0.774	0.7716	0.7721	0.595	0.583	0.582	0.583
	40	0.838	0.829	0.8277	0.8249	0.639	0.625	0.624	0.623
50	5	0.708	0.700	0.7034	0.7036	0.541	0.529	0.5309	0.531
	10	0.736	0.731	0.7317	0.7318	0.563	0.552	0.5522	0.552
	20	0.777	0.771	0.7721	0.7721	0.594	0.582	0.583	0.583
	40	0.830	0.827	0.825	0.8249	0.634	0.624	0.623	0.623

Ref.*= Pendhari *et al.* (2012)

The through-thickness variations of displacements and stresses for S=5, are shown in Fig. 5. The results of displacements and stresses obtained from TSDT are compared with available solutions given by Pendhari *et al.* (2012) and classical plate theory.

In-plane displacements show the different variations in upper and lower half of the FG plate indicating little departure in upper half compared to one given by semi-analytical solutions. Transverse displacement obtained using TSDT shows considerable departure from the semi-analytical solutions. In-plane normal stress $(\bar{\sigma}_{xx})$ show excellent variation with the semi-analytical solutions as seen from Table 4 and Fig. 5, whereas variation of $(\bar{\sigma}_{yy})$ shows little departure in the upper half compared to semi-analytical solution. The transverse shear stresses obtained by TSDT and their variations are in excellent agreement with those of semi-analytical solution.

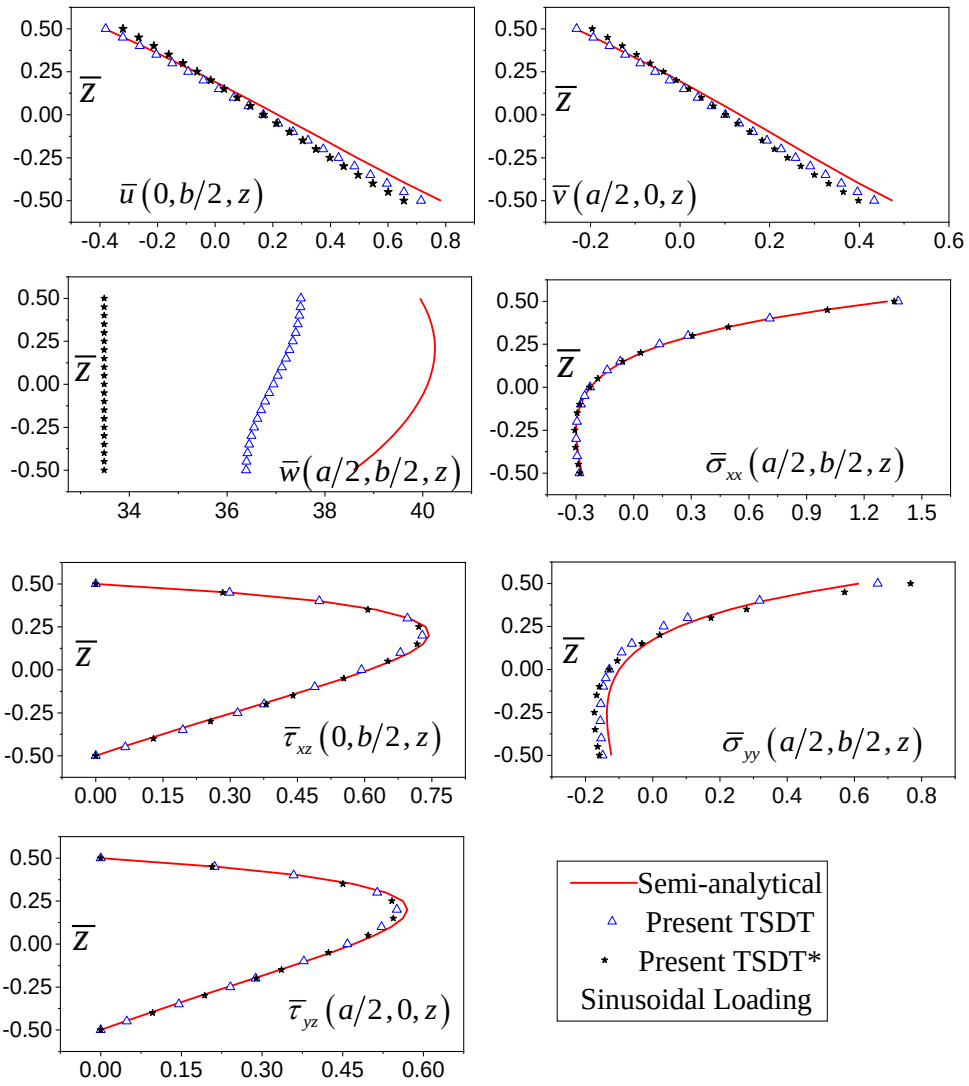

Fig. 5 Variation of normalized in-plane and transverse displacement ($\bar{u}$, $\bar{w}$), in-plane normal stresses ($\bar{\sigma}_{xx}$), in-plane and transverse shear stresses $(\bar{\tau}_{xy}, \bar{\tau}_{xz})$ for uniformly distributed loading condition in FG rectangular plate $(a/h = 5)$, $(b/a = 2)$ and E_r=10 for material

5. Conclusions

This study presents a bending analysis of the FG plate using trigonometric shear and normal deformation theory with $(\varepsilon_z = 0)$ and without $(\varepsilon_z \neq 0)$ transverse normal deformation effects. In this theory, in-plane displacements vary according to sine law, and transverse displacement varies according to cosine law through the thickness of the FG plate. The displacement field of the present refined theory is very simple, with six variables.

The boundary value problem of FG plate is derived using variational principle. The FG plate properties vary exponentially with respect to its thickness. The Navier's solution method is applied

to solve the boundary value problem for a simply supported FG plate and the results of present theory are compared with those of semi-analytical method. From results and discussion of this study following conclusions are drawn:

- The in-plane displacements increase with increase in E_r ratio irrespective of aspect ratio. Their variations across the thickness of FG plate show close agreement with those of semi-analytical solutions.
- Transverse displacements obtained using the current theory are reasonably accurate compared to the semi-analytical values. Theory including transverse normal strain is found to give more precise results than the theory without this effect.
- The in-plane and transverse stresses obtained using TSDT, which takes into account the transverse normal strain, are in excellent agreement with those of the semi-analytical solutions.
- In-plane normal stresses increase with increase in E_r ratio and decrease with increase in aspect ratio however, in-plane shear stress show reverse trend.
- The transverse shear stresses increase with the increase in E_r ratio and are independent of aspect ratio.
- The effect of transverse anisotropy of FGM is observed to influence the displacements and stresses significantly.

The numerical examples showed the efficiency of TSDT with transverse normal effect for FG plate under bending. The findings of this study can be used as benchmark solutions for comparison in future studies. In the near future, the theory will be applied to investigate thermal stresses in FG plates using TSDT.

References

Bakoura, A., Bourada, F., Bousahla, A.A., Tounsi, A., Benrahou, K.H., Tounsi, A., ... & Mahmoud, S.R. (2021), "Buckling analysis of functionally graded plates using HSD in conjunction with the stress function method", *Comput. Concrete*, **27**(1), 73-83. https://doi.org/10.12989/cac.2021.27.1.073.

Bennedjadi, M., Aldosari, S.M., Chikh, A., Kaci, A., Bousahla, A.A., Bourada, F., ... & Tounsi, A. (2023), "Visco-elastic foundation effect on buckling response of exponentially graded sandwich plates under various boundary conditions", *Geomech. Eng.*, **32**(2), 159-177. https://doi.org/10.12989/gae.2023.32.2.159.

Bhandari, M. and Purohit, K. (2014), "Static response of functionally graded material plate under transverse load for varying aspect ratio", *Int. J. Metal.*, **2014**, 1-11. https://doi.org/10.1155/2014/980563.

Bodaghi, M. and Saidi, A.R. (2010), "Levy-type solution for buckling analysis of thick functionally graded rectangular plates based on the higher-order shear deformation plate theory", *Appl. Math. Model.*, **34**(11), 3659-3673. https://doi.org/10.1016/j.apm.2010.03.016

Bouafia, K., Selim, M.M., Bourada, F., Bousahla, A.A., Bourada, M., Tounsi, A., ... & Tounsi, A. (2021), "Bending and free vibration characteristics of various compositions of FG plates on elastic foundation via quasi 3D HSDT model", *Steel Compos. Struct.*, **41**(4), 487-503. https://doi.org/10.12989/scs.2021.41.4.487.

Brischetto, S. and Carrera, E. (2010), "Advanced mixed theories for bending analysis of functionally graded plates", *Comput. Struct.*, **88**(23-24), 1474-1483. https://doi.org/10.1016/j.compstruc.2008.04.004.

Brischetto, S., Leetsch, R., Carrera, E., Wallmersperger, T. and Kröplin, B. (2008), "Thermo-mechanical bending of functionally graded plates", *J. Therm. Stress.*, **31**(3), 286-308. https://doi.org/10.1080/01495730701876775.

Carrera, E., Brischetto, S., Cinefra, M. and Soave, M. (2011), "Effects of thickness stretching in functionally graded plates and shells", *Compos. Part B: Eng.*, **42**(2), 123-133. https://doi.org/10.1016/j.compositesb.2010.10.005.

Carrera, E., Brischetto, S. and Robaldo, A. (2008), "Variable kinematic model for the analysis of functionally

graded material plates", *AIAA J.*, **46**(1), 194-203. https://doi.org/10.2514/1.32490

Chakraborty, A., Gopalakrishnan, S. and Reddy, J. (2003), "A new beam finite element for the analysis of functionally graded materials", *Int. J. Mech. Sci.*, **45**(3), 519-539 https://doi.org/10.1016/S0020-7403(03)00058-4.

Chakraverty, S. and Pradhan, K.K. (2014), "Free vibration of exponential functionally graded rectangular plates in thermal environment with general boundary conditions", *Aerosp. Sci. Technol.*, **36**, 132-156. https://doi.org/10.1016/j.ast.2014.04.005.

Chi, S.H. and Chung, Y.L. (2006), "Mechanical behavior of functionally graded material plates under transverse load-Part I: Analysis", *Int. J. Solid. Struct.*, **43**(13), 3657-3674. https://doi.org/10.1016/j.ijsolstr.2005.04.011.

Fazzolari, F.A. and Carrera, E. (2014a), "Refined hierarchical kinematics quasi-3D Ritz models for free vibration analysis of doubly curved FGM shells and sandwich shells with FGM core", *J. Sound Vib.*, **333**(5), 1485-1508. https://doi.org/10.1016/j.jsv.2013.10.030.

Fazzolari, F.A. and Carrera, E. (2014b), "Thermal stability of FGM sandwich plates under various through-the-thickness temperature distributions", *J. Therm. Stress.*, **37**(12), 1449-1481.https://doi.org/10.1080/01495739.2014.937251.

Filippi, M., Carrera, E. and Zenkour, A.M. (2015), "Static analyses of FGM beams by various theories and finite elements", *Compos. Part B: Eng.*, **72**, 1. https://doi.org/10.1016/j.compositesb.2014.12.004.

Garg, A., Belarbi, M.O., Li, L. and Tounsi, A. (2022), "Bending analysis of power-law sandwich FGM beams under thermal conditions", *Adv. Aircraft Spacecraft Sci.*, **9**(3), 243-261. https://doi.org/10.12989/aas.2022.9.3.243.

Ghugal, Y.M. and Sayyad, A.S. (2013), "Stress analysis of thick laminated plates using trigonometric shear deformation theory", *Int. J. Appl. Mech.*, **5**(1). https://doi.org/10.1142/S1758825113500038.

Guellil, M., Saidi, H., Bourada, F., Bousahla, A.A., Tounsi, A., Al-Zahrani, M.M., ... & Mahmoud, S.R. (2021), "Influences of porosity distributions and boundary conditions on mechanical bending response of functionally graded plates resting on Pasternak foundation", *Steel Compos. Struct.*, **38**(1), 1-15. https://doi.org/10.12989/scs.2021.38.1.001.

GulshanTaj, M.G., Chakrabarti, A. and Sheikh, A.H. (2013), "Analysis of functionally graded plates using higher order shear deformation theory", *Appl. Math. Model.*, **37**(18-19), 8484-8494. https://doi.org/10.1016/j.apm.2013.03.058.

Gupta, A. and Talha, M. (2017), "Nonlinear flexural and vibration response of geometrically imperfect gradient plates using hyperbolic higher-order shear and normal deformation theory", *Compos. Part B: Eng.*, **123**, 241-261. https://doi.org/10.1016/j.compositesb.2017.05.010.

Hachemi, H., Bousahla, A.A., Kaci, A., Bourada, F., Tounsi, A., Benrahou, K.H., ... & Mahmoud, S.R. (2021), "Bending analysis of functionally graded plates using a new refined quasi-3D shear deformation theory and the concept of the neutral surface position", *Steel Compos. Struct.*, **39**(1), 51-64. https://doi.org/10.12989/cac.2021.39.1.051.

Hadji, M., Bouhadra, A., Mamen, B., Menasria, A., Bousahla, A.A., Bourada, F., ... & Tounsi, A. (2023), "Combined influence of porosity and elastic foundation parameters on the bending behavior of advanced sandwich structures", *Steel Compos. Struct.*, **46**(1), 1-13. https://doi.org/10.12989/scs.2023.46.1.001.

Jha, D.K., Kant, T. and Singh, R.K. (2013), "Stress analysis of transversely loaded functionally graded plates with a higher order shear and normal deformation theory", *J. Eng. Mech.*, **139**(12), 1663-1680. https://doi.org/10.1061/(ASCE)EM.1943-7889.0000601.

Kant, T., Jha, D.K. and Singh, R.K. (2014), "A higher-order shear and normal deformation functionally graded plate model: Some recent results", *Acta Mechanica*, **225**(10), 2865-2876. https://doi.org/10.1007/s00707-014-1213-2.

Khan, T., Zhang, N. and Akram, A. (2019), "State of the art review of functionally graded materials" , *2019 2nd International Conference on Computing*, *Mathematics and Engineering Technologies (iCoMET)*, 1-9.

Kulkarni, K., Singh, B.N. and Maiti, D.K. (2015), "Analytical solution for bending and buckling analysis of functionally graded plates using inverse trigonometric shear deformation theory", *Compos. Struct.*, **134**, 147-157. https://doi.org/10.1016/j.compstruct.2015.08.060.

Lü, C.F., Chen, W.Q., Xu, R.Q. and Lim, C.W. (2008), "Semi-analytical elasticity solutions for bi-directional functionally graded beams", *Int. J. Solid. Struct.*, **45**(38), 258-275. https://doi.org/10.1016/j.ijsolstr.2007.07.018.

Mashat, D.S., Carrera, E., Zenkour, A.M., Al Khateeb, S.A. and Filippi, M. (2014), "Free vibration of FGM layered beams by various theories and finite elements", *Compos. Part B: Eng.*, **59**, 269-278. https://doi.org/10.1016/j.compositesb.2013.12.008.

El Meiche, N., Tounsi, A., Ziane, N. and Mechab, I. (2011), "A new hyperbolic shear deformation theory for buckling and vibration of functionally graded sandwich plate", *Int. J. Mech. Sci.*, **53**(4), 237-247. https://doi.org/10.12989/eas.2018.14.2.103.

Merazka, B., Bouhadra, A., Menasria, A., Selim, M.M., Bousahla, A.A., Bourada, F., ... & Al-Zahrani, M.M. (2021), "Hygro-thermo-mechanical bending response of FG plates resting on elastic foundations", *Steel Compos. Struct.*, **39**(5), 631-643. https://doi.org/10.12989/scs.2021.39.5.631.

Merdaci, S. and Belghoul, H. (2019), "High-order shear theory for static analysis of functionally graded plates with porosities", *Comptes Rendus Mécanique*, **347**(3), 207-217. https://doi.org/10.1016/j.crme.2019.01.001.

Mudhaffar, I.M., Tounsi, A., Chikh, A., Al-Osta, M.A., Al-Zahrani, M.M. and Al-Dulaijan, S.U. (2021), "Hygro-thermo-mechanical bending behavior of advanced functionally graded ceramic metal plate resting on a viscoelastic foundation", *Struct.*, **33**, 2177-2189. https://doi.org/10.1016/j.istruc.2021.05.090.

Na, K.S. and Kim, J.H. (2006), "Nonlinear bending response of functionally graded plates under thermal loads", *J. Therm. Stress.*, **29**(3), 245-261. https://doi.org/10.1080/01495730500360427.

Neves, A.M.A., Ferreira, A.J.M., Carrera, E., Cinefra, M., Roque, C.M.C., Jorge, R.M.N. and Soares, C.M.M. (2012), "A quasi-3D hyperbolic shear deformation theory for the static and free vibration analysis of functionally graded plates", *Compos. Struct.*, **94**(5), 1814-1825. https://doi.org/10.1016/j.compstruct.2011.12.005.

Neves, A.M.A., Ferreira, A.J.M., Carrera, E., Cinefra, M., Roque, C.M.C., Jorge, R.M.N. and Soares, C.M. (2013), "Static, free vibration and buckling analysis of isotropic and sandwich functionally graded plates using a quasi-3D higher-order shear deformation theory and a meshless technique", *Compos. Part B: Eng.*, **44**(1), 657-674. https://doi.org/10.1016/j.compositesb.2012.01.089.

Nguyen, T.K. (2015), "A higher-order hyperbolic shear deformation plate model for analysis of functionally graded materials", *Int. J. Mech. Mater. Des.*, **11**(2), 203-219. https://doi.org/10.1007/s10999-014-9260-3.

Nguyen, T.K., Sab, K. and Bonnet, G. (2008), "First-order shear deformation plate models for functionally graded materials", *Compos. Struct.*, **83** (1), 25-36. https://doi.org/10.1016/j.compstruct.2007.03.004.

Pendhari, S.S., Kant, T., Desai, Y.M. and Subbaiah, C.V. (2012), "Static solutions for functionally graded simply supported plates", *Int. J. Mech. Mater. Des.*, **8**(1), 51-69. https://doi.org/10.1007/s10999-011-9175-1.

Pradhan, P., Sutar, M.K. and Pattnaik, S. (2019), "A state of the art in functionally graded materials and their analysis", *Mater. Today: Proc.*, **18**, 3931-3936. https://doi.org/https://doi.org/10.1016/j.matpr.2019.07.333.

Praveen, G.N. and Reddy, J.N. (1998), "Nonlinear transient thermoelastic analysis of functionally graded ceramic-metal plates", *Int. Solid. Struct.*, **35**(33), 4457-4476. https://doi.org/10.1016/S0020-7683(97)00253-9.

Reddy, J. (2000), "Analysis of functionally graded plates", *Int. J. Numer. Meth. Eng.*, **47**(1-3), 663-684. https://doi.org/10.1002/(SICI)1097-0207(20000110/30)47:1/3<663::AID-NME787>3.0.CO;2-8.

Saleh, B., Jiang, J., Fathi, R., Al-hababi, T., Xu, Q., Wang, L., ... & Ma, A. (2020), "30 Years of functionally graded materials: An overview of manufacturing methods, applications and future challenges", *Compos. Part B: Eng.*, **201**, 108376. https://doi.org/10.1016/j.compositesb.2020.108376.

Sankar, B.V. (2001), "An elasticity solution for functionally graded beams", *Compos. Sci. Technol.*, **61**(5), 689-696. https://doi.org/10.1016/S0266-3538(01)00007-0.

Sayyad, A.S. and Ghugal, Y.M. (2014), "A new shear and normal deformation theory for isotropic, transversely isotropic, laminated composite and sandwich plates", *Int. J. Mech. Mater. Des.*, **10**(3), 247-267. https://doi.org/10.1007/s10999-014-9244-3.

Sayyad, A.S. and Ghugal, Y.M. (2016), "Cylindrical bending of multilayered composite laminates and sandwiches", *Adv. Aircraft Spacecraft Sci.*, **3**(2), 113-148. https://doi.org/10.12989/aas.2016.3.2.113.

Sayyad, A.S. and Ghugal, Y.M. (2017), "A unified shear deformation theory for the bending of isotropic, functionally graded, laminated and sandwich beams and plates", *Int. J. Appl. Mech.*, **09**(01), 1750007. https://doi.org/10.1142/S1758825117500077.

Shahrjerdi, A., Mustapha, F., Bayat, M., Sapuan, S.M., Zahari, R. and Shahzamanian, M.M. (2011), "Natural frequency of F.G. rectangular plate by shear deformation theory", *IOP Conf. Ser.: Mater. Sci. Eng.*, **17**(1), 012008 https://doi.org/10.1088/1757-899X/17/1/012008.

Srividhya, S., Kumar, B., Gupta, R.K. and Rajagopal, A. (2019), "Nonlinear analysis of FGM plates using generalised higher order shear deformation theory", *Int. J. Mater. Struct. Integr.*, **13**(1-3), 3-15. https://doi.org/10.1504/IJMSI.2019.100381.

Srividhya, S., Raghu, P., Rajagopal, A. and Reddy, J. (2018), "Nonlocal nonlinear analysis of functionally graded plates using third-order shear deformation theory", *Int. J. Eng. Sci.*, **125**, 1-22. https://doi.org/10.1016/j.ijengsci.2017.12.006.

Swami, S. K. and Ghugal, Y. M. (2021), "Thermoelastic bending analysis of laminated plates subjected to linear and nonlinear thermal loads", *Adv. Aircraft Spacecraft Sci.*, **8**(3), 213-237. https://doi.org/10.12989/aas.2021.8.3.213.

Swaminathan, K., Naveenkumar, D. T., Zenkour, A. M. and Carrera, E. (2015), "Stress, vibration and buckling analyses of FGM plates-A state-of-the-art review", *Compos. Struct.*, **120**, 10-31. https://doi.org/10.1016/j.compstruct.2014.09.070.

Tahir, S. I., Tounsi, A., Chikh, A., Al-Osta, M. A., Al-Dulaijan, S. U. and Al-Zahrani, M. M. (2022), "The effect of three-variable viscoelastic foundation on the wave propagation in functionally graded sandwich plates via a simple quasi-3D HSDT", *Steel Compos. Struct.*, **42**(4), 501. https://doi.org/10.12989/scs.2022.42.4.501.

Woodward, B. and Kashtalyan, M. (2011), "Three-dimensional elasticity solution for bending of transversely isotropic functionally graded plates", *Eur. J. Mech.-A/Solid.*, **30**(5), 705-718. https://doi.org/10.1016/j.euromechsol.2011.04.00.

Yadav, S., Damse, S., Pendhari, S., Sangle, K. and Sayyad, A.S. (2022), "Comparative studies between Semi-analytical and shear deformation theories for functionally graded beam under bending", *Forc. Mech.*, **8**, 100111. https://doi.org/10.1016/j.finmec.2022.100111.

Yadav, S., Pandare, P., Pendhari, S., Sangle, K. and Ghugal, Y.M. (2023a), "Static analysis of an exponentially varying functionally graded beam using trigonometric shear deformation theory", *Compos.: Mech. Comput. Appl.*, **14**(3), 1-23. https://doi.org/10.1615/CompMechComputApplIntJ.2023047080.

Yadav, S.S., Sangle, K.K., Shinde, S.A., Pendhari, S.S. and Ghugal, Y.M. (2023b), "Bending analysis of FGM plates using sinusoidal shear and normal deformation theory", *Forc. Mech.*, **11**, 100185 https://doi.org/10.1016/j.finmec.2023.100185.

Zaitoun, M.W., Chikh, A., Tounsi, A., Al-Osta, M.A., Sharif, A., Al-Dulaijan, S.U. and Al-Zahrani, M.M. (2022), "Influence of the visco-Pasternak foundation parameters on the buckling behavior of a sandwich functional graded ceramic-metal plate in a hygrothermal environment", *Thin Wall. Struct.*, **170**, 108549. https://doi.org/10.1016/j.tws.2021.108549.

Zenkour, A.M. (2005), "A comprehensive analysis of functionally graded sandwich plates: Part 1-Deflection and stresses", *Int. J. Solid. Struct.*, **42**(18-19), 5224-5242. https://doi.org/10.1016/j.ijsolstr.2005.02.015.

Zenkour, A.M. (2006), "Generalized shear deformation theory for bending analysis of functionally graded plates", *Appl. Math. Model.*, **30**(1), 67-84. https://doi.org/10.1016/j.apm.2005.03.009.

Zhang, H., Jiang, J.Q. and Zhang, Z.C. (2014), "Three-dimensional elasticity solutions for bending of generally supported thick functionally graded plates", *Appl. Math. Mech.*, **35**(11), 1467-1478. https://doi.org/10.1007/s10483-014-1871-7.

Zhong, Y., Li, R., Liu, Y. and Tian, B. (2009), "On new symplectic approach for exact bending solutions of moderately thick rectangular plates with two opposite edges simply supported", *Int. J. Solid. Struct.*, **46**(11-12), 2506-2513. https://doi.org/10.1016/j.ijsolstr.2009.02.001.

Appendix

The elements of stiffness matrix $[K]$ in Eq. (19) are given as follows

$$K_{11} = A_{11}\alpha^2 + A_{66}\beta^2, K_{12} = (A_{12} + A_{66})\alpha\beta,$$
$$K_{13} = -[B_{11}\alpha^3 + (B_{12} + 2B_{66})\alpha\beta^2],$$
$$K_{14} = As_{11}\alpha^2 + As_{66}\beta^2,$$
$$K_{15} = (As_{12} + As_{66})\alpha\beta, K_{16} = \left(\frac{\pi}{h}\right) As_{13}\alpha,$$
$$K_{22} = A_{66}\alpha^2 + A_{22}\beta^2,$$
$$K_{23} = -[B_{22}\beta^3 + (B_{12} + 2B_{66})\alpha^2\beta],$$
$$K_{24} = (As_{12} + As_{66})\alpha\beta,$$
$$K_{25} = As_{66}\alpha^2 + As_{22}\beta^2,$$
$$K_{26} = \frac{\pi}{h} As_{23}\beta,$$
$$K_{33} = D_{11}\alpha^4 + 2(D_{12} + 2D_{66})\alpha^2\beta^2 + D_{22}\beta^4,$$
$$K_{34} = -[Bs_{11}\alpha^3 + (Bs_{12} + 2Bs_{66})\alpha\beta^2],$$
$$K_{35} = -[Bs_{22}\beta^3 + (Bs_{12} + 2Bs_{66})\alpha^2\beta],$$
$$K_{36} = -\left(\frac{\pi}{h}\right)(Bs_{13}\alpha^2 + Bs_{23}\beta^2),$$
$$K_{44} = (Ass_{11}\alpha^2 + Ass_{66}\beta^2 + Acc_{55}),$$
$$K_{45} = (Ass_{12} + Ass_{66})\alpha\beta,$$
$$K_{46} = \left(\left(\frac{\pi}{h}\right) Ass_{13} + \left(\frac{h}{\pi}\right) Acc_{55}\right)\alpha,$$
$$K_{55} = (Ass_{66}\alpha^2 + Ass_{11}\beta^2 + Acc_{44}),$$
$$K_{56} = \left(\left(\frac{\pi}{h}\right) Ass_{23} + \left(\frac{h}{\pi}\right) Acc_{44}\right)\beta,$$
$$K_{66} = \left(\left(\frac{h}{\pi}\right)^2 Acc_{55}\alpha^2 + \left(\frac{h}{\pi}\right)^2 Acc_{44}\beta^2 + \left(\frac{\pi}{h}\right)^2 Ass_{33}\right)$$